NACA RM L53J15

NACA

RESEARCH MEMORANDUM

THE INFLUENCE OF THE CONTROL-SURFACE-SERVO NATURAL FREQUENCY UPON THE TRANSIENT CHARACTERISTICS OF A FLIGHT-PATH-ANGLE CONTROL SYSTEM INCORPORATING A SUPERSONIC MISSILE

By Anthony L. Passera and Thomas F. Bridgland, Jr.

Langley Aeronautical Laboratory
Langley Field, Va.

NATIONAL ADVISORY COMMITTEE
FOR AERONAUTICS
WASHINGTON

December 10, 1953
Declassified October 18, 1956

NATIONAL ADVISORY COMMITTEE FOR AERONAUTICS

RESEARCH MEMORANDUM

THE INFLUENCE OF THE CONTROL-SURFACE-SERVO NATURAL FREQUENCY UPON THE TRANSIENT CHARACTERISTICS OF A FLIGHT-PATH-ANGLE CONTROL SYSTEM INCORPORATING A SUPERSONIC MISSILE

By Anthony L. Passera and Thomas F. Bridgland, Jr.

SUMMARY

A theoretical investigation has been made to determine the effects of control-surface-servo natural frequency upon the transient characteristics - response time, attitude accuracy, peak rate and total volume of oil flow through the servo, and maximum normal acceleration of the airframe - of a flight-path-angle control system for three values of the airframe static margin and five flight conditions.

The plots of transient characteristics against control-surface-servo natural frequency show that no appreciable improvement in response time is achieved by increasing the control-surface-servo natural frequency beyond 50 radians/sec. For the larger airframe static margins considered in the investigation, use of servo natural frequencies in the neighborhood of 70 radians/sec yields a maximum total volume of oil flow through the servo, whereas an almost linear increase in peak rate of oil flow is effected by increase in servo natural frequency with the highest peak rates at a given frequency being exhibited by the systems having the larger airframe static margins.

INTRODUCTION

As part of a general research program, the Langley Pilotless Aircraft Research Division has been conducting a theoretical investigation of a supersonic missile configuration incorporated in various types of automatic

control systems. The present investigation is concerned with analysis of a flight-path-angle control system incorporating this missile.

The effect of control-surface-servo natural frequency upon the transient characteristics - response time, attitude accuracy, peak rate and total volume of oil flow through the servo, and maximum normal acceleration of the airframe - was investigated for three values of airframe static margin and for five flight conditions.

The analysis was executed by simulation of the dynamic components of the control system on the Reeves Electronic Analog Computer (REAC) at the Langley Laboratory. The adjustable gains of the control system were set at one flight condition and held constant for the other flight conditions. These gains were adjusted so as to yield a minimum error response between the pitch-attitude angle of the airframe and a unit step input to the flight-path-angle control system. The analysis was performed under the assumption that direct sensing of flight-path angle was possible.

SYMBOLS

$\bar{c}$	mean aerodynamic chord, 1.77 ft
E_r	output of rate gyro proportional to $\dot{\theta}_o$, deg
g	acceleration due to gravity, 32.2 ft/sec^2
K	control-surface-servo static gain, deg/deg
K_g	static gain constant of transfer function, $n_o/\dot{\theta}_o$, g units/deg/sec
K_r	static gain constant of transfer function, $E_r/\dot{\theta}_o$, deg/deg/sec
n_o	normal acceleration of airframe, g units
M	Mach number
q	dynamic pressure, lb/sq ft
S	total wing area, 4.1 sq ft
s	Laplace transform variable

x_{sm}	static margin, fraction of $\bar{c}$
t	time, sec
W	weight of airframe, lb
α_o	angle of attack, deg
γ_i	desired flight-path angle of control system, deg
γ_o	flight-path-angle output of control system, deg
δ	control-surface deflection, deg
ϵ	flight-path-angle error signal, $\gamma_i - \gamma_o$, deg
ϵ_1	inner-loop error signal, $\epsilon - E_r$, deg
ϵ_2	error signal, $\gamma_i + \alpha_o$, deg
ϵ_θ	pitch-attitude-angle error signal, $\gamma_i - \theta_o$, deg
ζ	quadratic damping ratio of control-surface servo
θ_o	pitch-attitude angle of airframe, deg
ω_n	control-surface-servo undamped natural frequency, radians/sec
C_L	lift coefficient, Lift/qS
$C_{L_\alpha} = \frac{\partial C_L}{\partial \alpha}$	
$C_{L_\delta} = \frac{\partial C_L}{\partial \delta}$	
$\int \lvert \epsilon_\theta(t) \rvert dt$	measure of attitude accuracy, deg-sec
$\int \lvert \epsilon(t) \rvert dt$	measure of flight-path accuracy, deg-sec

Subscripts:

i input

o output

A dot over a symbol indicates a derivative with respect to time.

DESCRIPTION OF CONTROL SYSTEM

Major Components

The block diagram of the flight-path-angle control system under consideration in this investigation is shown as follows:

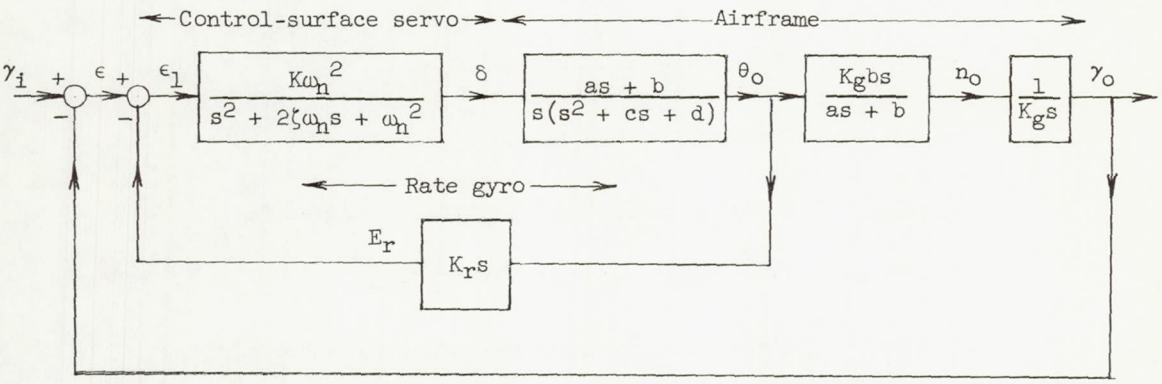

The missile considered in this analysis, as shown in figure 1, is a symmetric and cruciform configuration having a fineness ratio of approximately 16. The wings and canard fins have a delta plan form with the leading edges swept back 60° and with a modified double-wedge cross section. The horizontal canard fins provide longitudinal control and auxiliary damping, the latter through the action of a rate gyro and the control-surface servo.

The rate gyro is assumed to be a perfect differentiator with the transfer function

$$\frac{E_r}{\theta_o}(s) = K_r s$$

Longitudinal control deflections are produced by the action of a hydraulic servo, of the type described in reference 1, having the transfer function

$$\frac{\delta}{\epsilon_1}(s) = \frac{K\omega_n^2}{s^2 + 2\zeta\omega_n s + \omega_n^2}$$

The four values of the control-surface-servo natural frequency ω_n considered in this investigation are as follows: $\omega_n = 30$, 50, 70, and 140 with $\zeta = 0.5$.

The transfer functions relating θ_o to δ, n_o to θ_o, and γ_o to n_o, derived from the airframe equations of motion assuming two degrees of freedom longitudinally and small disturbances from level flight, are, respectively,

$$\frac{\theta_o}{\delta}(s) = \frac{as + b}{s(s^2 + cs + d)}$$

$$\frac{n_o}{\theta_o}(s) = \frac{K_g bs}{as + b}$$

$$\frac{\gamma_o}{n_o}(s) = \frac{1}{K_g s}$$

The coefficients of these transfer functions are functions of the airframe stability derivatives tabulated in reference 2. Values of a, b, c, d, and K_g for the various flight conditions investigated are listed in table I.

Method of Sensing Flight-Path Angle

In the ensuing analysis, direct feedback of γ_o is assumed. Although such direct sensing of flight-path angle is not physically realizable, it may be accomplished indirectly in the following manner, based on the relation $\gamma_o = \theta_o - \alpha_o$. If the angle of attack α_o is sensed by, for example, an angle-of-attack vane and the corresponding signal representing α_o is added to the input γ_i, the error signal ϵ_2, is produced

as shown in the following diagram:

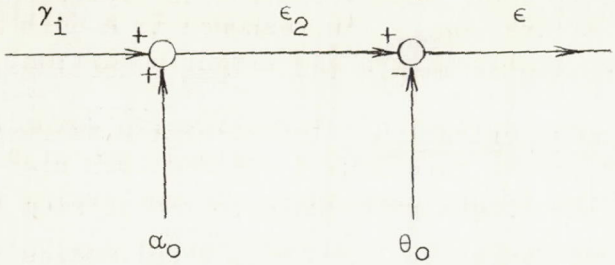

Subtracting the pitch-attitude-angle signal θ_o from ϵ_2 gives the error signal $\epsilon = \gamma_i + \alpha_o - \theta_o$. But, $\alpha_o - \theta_o = -\gamma_o$. Hence, $\epsilon = \gamma_i - \gamma_o$. This error signal ϵ is then used as an input to the control-surface servo just as in the system considered in this paper.

Alternately, α_o may be obtained as the output of an accelerometer sensitive to normal acceleration n_o, since, for $C_{L_\delta} = 0$, $\alpha_o = \frac{57.3W}{qSC_{L_\alpha}} n_o$. A disadvantage of this means of obtaining α_o is that the accelerometer static gain, whose value will be the ratio $57.3W/qSC_{L_\alpha}$, must be sensitive to changes in C_{L_α} and in the dynamic pressure q. The extreme values of the ratio $57.3W/qSC_{L_\alpha}$ for the missile configuration considered herein are for sea-level flight. A variation in Mach number from 1.0 to 2.0 produces a variation in this ratio from 0.476° per g unit to 0.154° per g unit.

ANALYSIS PROCEDURE

The purpose of this investigation is to determine the effect of the control-surface-servo natural frequency upon the transient characteristics of the control system with variations in the airframe static margin for various flight conditions.

Compact control systems demand low values of total oil consumption and peak rate of oil consumption by the servo. Following reference 1, these quantities are taken as being proportional to the total control-surface travel $\int|d\delta|$ and $\dot{\delta}_{max}$, respectively, and are used as a basis of comparison for the systems in this investigation.

The missile of this analysis has a design load limit of 25g; hence, input amplitudes causing the missile acceleration response to exceed this

limit are not permissible. In order to obtain an indication of the range of permissible step input amplitudes for the systems of this analysis, the peak accelerations $n_{o_{max}}$ in response to a unit step γ_i input are compared for each static margin and flight condition.

Gain adjustment criterion.- Investigation demonstrated that the gain adjustment criterion of reference 1 yielded such high values of $\dot{\delta}_{max}$ and $n_{o_{max}}$ for the flight-path-angle control system that this criterion was not considered feasible. For the present analysis, the gains K and K_r are considered to be optimum when their values are such as to minimize $\int|\epsilon_\theta(t)|dt$ where $\epsilon_\theta = \gamma_i - \theta_o$. Adjustment of the gains in this manner permits the control system to operate within the practical limits of existing servos and within the design load limit of the missile for a broader range of amplitude of the input γ_i. For this investigation, low values of $\int|\epsilon_\theta(t)|dt$ are taken as being equivalent to high attitude accuracy.

A further advantage of the application of the foregoing criterion to the flight-path-angle control system may be that, if the control system were used in conjunction with some type of seeker, the missile would be enabled to point more accurately toward the target aircraft in virtue of the minimized attitude error, thus yielding a greater probability of keeping the target within the field of view of the seeker.

Gain adjustment technique.- The procedure for obtaining the gains K and K_r of the control system was performed on the REAC for each static margin and each value of the control-surface-servo natural frequency in the following manner. The flight condition $M = 1.6$ at sea level was chosen for the minimization condition. The rate-gyro gain K_r was set at a given value and the control-surface-servo gain K varied over a range of discrete values. At each value of K, the value of $\int|\epsilon_\theta(t)|dt$ resulting from a unit step input was tabulated. The integration of $|\epsilon_\theta(t)|$ was extended over the interval from $t = 0$ to, effectively, $t \rightarrow \infty$. A plot was then made of $\int|\epsilon_\theta(t)|dt$ against K for the particular value of K_r used. K_r was then adjusted to a new value and the foregoing process repeated. As is shown for a typical case in figure 2, each of the curves plotted against K exhibits a well-defined minimum. During the process of obtaining these curves, care was taken to use a sufficient range of values of K to locate this minimum closely. It was also established that this minimum was unique, within the REAC voltage limits, for each curve.

By considering $\int|\epsilon_\theta(t)|dt$ as a function of the variables K and K_r, figure 2 may be viewed as the parametric contour representation

of the surface $\int|\epsilon_\theta(t)|dt = F(K,K_r)$ with K_r as parameter. The minimum of this surface is immediately obtained from the contour of parameter $K_r = 0.015$ in the case shown. Values of K and K_r for which $\int|\epsilon_\theta(t)|dt$ is a minimum at $M = 1.6$ for sea-level flight are tabulated for various values of static margin and ω_n in table II.

Summarization of $\gamma_o(t)$ Transient Data

In the analysis, minimization of $\int|\epsilon_\theta(t)|dt$ yielded $\gamma_o(t)$ transient responses that exhibited, in general, a slow exponential rise with well-damped oscillatory modes as shown in figure 3, which contains a set of typical transient responses of the system as obtained from the REAC. For this type of motion, the variation of the measure of flight-path accuracy $\int|\epsilon(t)|dt$ with ω_n is usually reflected in the variation of response time with ω_n. This latter characteristic, response time, is used as a basis of comparison for the $\gamma_o(t)$ transient data obtained in this investigation. Here the definition of response time is that given in reference 1. It is that time beyond which a transient response to a step input remains within 5 percent of its steady-state value.

RESULTS AND DISCUSSION

The values of K and K_r given in table II were substituted successively in the system transfer functions and plots obtained of $\gamma_o(t)$, $\delta(t)$, $\dot{\delta}(t)$, and $n_o(t)$ in response to a unit step γ_i input for each static margin and each flight condition. Numerical values of $\int|\epsilon_\theta(t)|dt$ were also obtained for each of these conditions. These data are summarized as plots of response time, $\int|\epsilon_\theta(t)|dt$, $\int|d\delta|$, $\dot{\delta}_{max}$, and $n_{o_{max}}$ in figures 4 to 8, inclusive.

Response Time

Figure 4 indicates for most cases a gradual decrease in $\gamma_o(t)$ response time with increasing control-surface-servo natural frequency. This decrease is of an asymptotic nature with, in general, little improvement in response time being noted for frequencies greater than $\omega_n = 50$. As noted in the preceding section, a similar variation of the measure of flight-path accuracy $\int|\epsilon(t)|dt$ with frequency might be expected.

In figure 4 it is further observed that, except for the flight conditions $M = 1.2$ at sea level and $M = 1.6$ at 40,000 feet, variation in static margin for a given Mach number and altitude produced variation of response time of less than 0.2 second for frequencies greater than $\omega_n = 50$. For the aforementioned exceptional cases, the large and intermediate static margins produced transients with the least response time for $M = 1.2$ at sea level and the intermediate static margin produced the least response time for $M = 1.6$ at 40,000 feet over the entire frequency range.

Figure 4 also indicates that for a given static margin the response time decreases with increasing Mach number for flight at sea level over the entire frequency range. Also, for a Mach number of 1.6, increase in altitude increases response time.

Attitude Accuracy

Figure 5 presents trends for attitude accuracy similar to those for response time. Increase in control-surface-servo natural frequency is accompanied by an increase in attitude accuracy which generally is considerable for frequencies lower than $\omega_n = 70$ but which becomes negligible for frequencies greater than $\omega_n = 70$.

As further shown by figure 5, variation in Mach number from 1.2 to 2.0 at sea level produces the least variation in attitude accuracy for a large static margin and the greatest variation for a small static margin. However, the roles of these two static margins are reversed for an increase in altitude from sea level to 40,000 feet at $M = 1.6$. For this case, attitude accuracy exhibits the greatest variation, at low values of ω_n, for a large static margin and the least variation for a small static margin. At frequencies greater than $\omega_n = 70$, all static margins manifest about the same degree of variation of attitude accuracy with altitude.

The effect of variation in static margin for various flight conditions is also indicated in figure 5. At $M = 1.2$, the large static-margin system possesses the greatest attitude accuracy. For the higher Mach numbers, the system having the intermediate static margin is the most accurate for the midrange frequencies, being equalled in this respect by the large static-margin system at higher frequencies. For the higher frequencies, the large static-margin system is the most accurate at all altitudes.

Total Volume of Oil Flow

It is seen in figure 6 that, for the intermediate and large static margins, an increase in control-surface-servo natural frequency from $\omega_n = 30$ to $\omega_n = 70$ caused a decided increase in total volume of oil flow required, with maximum total volume required being attained at $\omega_n = 70$. This maximum is particularly pronounced for the large static-margin system. The small static-margin system exhibited a fairly constant total volume demand over the entire frequency range.

In general, figure 6 shows that the effect of increase in Mach number at sea level was an increase in total volume of flow, particularly at the middle of the frequency range, with this quantity tending toward the same value for all Mach numbers at the higher frequencies. The foregoing effects become more obvious with increasing static margin. Increase in altitude at $M = 1.6$ for the large static margin had the reverse effect, generally tending to reduce the total volume of oil flow.

Figure 6 further indicates that, for all Mach numbers and altitudes, increase in static margin effected a corresponding increase in total volume of flow, the system having the small static margin demanding the least total volume and the system with the large static margin demanding the most.

Peak Rate of Oil Flow

Figure 7 presents a summary of data for the peak rate of oil flow for only one flight condition. For other Mach numbers and altitudes, the values of the points shown in this figure differ by only a few percent. The outstanding feature of this figure is that for each static margin the peak rate of oil flow exhibits an almost linear increase with control-surface-servo natural frequency. It is also to be observed that increasing the airframe static margin increases the peak rate of flow over the entire frequency range.

Maximum Normal Acceleration

In figure 8 it is seen that $n_{o_{max}}$ exhibits a generally decreasing trend with increasing control-surface-servo natural frequency except for the small static-margin system for which $n_{o_{max}}$ manifests a slight rise for frequencies greater than $\omega_n = 70$.

An additional observation is that $n_{o_{max}}$ increases with increasing Mach number and decreases with increasing altitude. Also, $n_{o_{max}}$ generally increases with static margin, this increase being, however, at 2.5g.

Figure 8 also shows that for no flight condition did $n_{o_{max}}$ exceed 8g for a unit step γ_i input. Hence, for this missile at $M = 2.0$ in sea-level flight, the maximum-step-input γ_i amplitude would have to be restricted to be less than approximately 3°.

CONCLUSIONS

A theoretical investigation has been made to determine the effects of control-surface-servo natural frequency upon the transient characteristics of a flight-path-angle control system for three values of the airframe static margin and five flight conditions. In view of the results indicated by the transient characteristics in the preceding section, the following conclusions may be drawn:

1. Negligible improvement in response time is achieved through the use of servos having a natural frequency greater than 50 radians/sec. At frequencies greater than 50 radians/sec, variation in static margin at a given flight condition has a negligible effect upon the flight-path-angle transient response time with the exception of flight at a Mach number of 1.6 at 40,000 feet and at a Mach number of 1.2 at sea level. For a given static margin, a decrease in the flight-path-angle transient response time is effected by an increase in Mach number for sea-level flight and by a decrease in altitude for a Mach number of 1.6.

2. Increase in attitude accuracy is negligible for increases beyond 70 radians/sec in the servo natural frequency. Increasing the static margin diminishes the variation in attitude accuracy effected by changes in Mach number for sea-level flight over the entire frequency range.

3. Although the small static-margin system manifests an almost constant demand on total volume of oil flow, the large and intermediate static-margin systems exhibit an increasing total volume demand with increasing servo natural frequency to 70 radians/sec, after which it decays. For a given static margin, decreasing the Mach number at sea level or increasing the altitude at a Mach number of 1.6 has the effect of reducing the total volume of oil flow required. For a given flight condition, reduction of static margin effects a reduction in total volume of flow required.

4. The peak rate of oil flow displays an almost linear increase with servo natural frequency for all static margins and all flight conditions. Variations in flight condition at a given static margin has no discernible effect upon the peak rate of flow. Peak rate of flow increases with static margin for all flight conditions.

5. Maximum normal acceleration of the airframe exhibits a generally decreasing trend with increasing servo natural frequency except for the small static margin which exhibits a slight increase for frequencies greater than 70 radians/sec. For a given static margin, maximum normal acceleration increases with Mach number for sea-level flight and decreases with increasing altitude at a Mach number of 1.6. For a given flight condition, maximum normal acceleration increases with static margin.

Langley Aeronautical Laboratory,
National Advisory Committee for Aeronautics,
Langley Field, Va., September 29, 1953.

REFERENCES

1. Passera, Anthony L., and Nason, Martin L.: The Effect of Control-Surface-Servo Natural Frequency on the Dynamic Performance Characteristics of an Acceleration Control System Applied to a Supersonic Missile. NACA RM L53G23a, 1953.

2. Seaberg, Ernest C., and Smith, Earl F.: Theoretical Investigation of an Automatic Control System With Primary Sensitivity to Normal Accelerations as Used To Control a Supersonic Canard Missile Configuration. NACA RM L51D23, 1951.

TABLE I.- AIRFRAME TRANSFER FUNCTION COEFFICIENTS FOR VARIOUS VALUES OF STATIC MARGIN, MACH NUMBER, AND ALTITUDE

[$\bar{c}$ = 1.77 feet]

Mach number	Altitude, ft	a	b	c	d	K_g, g units/deg/sec
$x_{sm} = 0.094\bar{c}$ at M = 1.6						
1.2	Sea level	407	1,587	6.44	209	0.726
1.6	Sea level	621	2,797	7.76	230	.968
1.6	10,000	425	1,357	5.56	155	.934
1.6	40,000	115	110	1.67	41	.842
2.0	Sea level	797	4,240	9.35	164	1.128
$x_{sm} = 0.294\bar{c}$ at M = 1.6						
1.2	Sea level	407	1,587	6.64	518	0.726
1.6	Sea level	621	2,797	8.03	690	.968
1.6	10,000	425	1,357	5.71	469	.934
1.6	40,000	115	110	1.71	125	.842
2.0	Sea level	797	4,240	9.23	871	1.218
$x_{sm} = 0.564\bar{c}$ at M = 1.6						
1.2	Sea level	407	1,587	7.15	920	0.726
1.6	Sea level	621	2,797	8.64	1319	.968
1.6	10,000	425	1,357	6.14	890	.934
1.6	40,000	115	110	1.84	241	.842
2.0	Sea level	797	4,240	9.86	1786	1.218

TABLE II.- VALUES OF K AND K_r FOR MINIMIZATION OF $\int|\epsilon_\theta(t)|dt$ AT M = 1.6 AND SEA LEVEL TABULATED AGAINST CONTROL-SURFACE-SERVO NATURAL FREQUENCY FOR THREE STATIC MARGINS

ω_n	K	K_r
$x_{sm} = 0.094\bar{c}$ at M = 1.6		
30	0.278	0.060
50	.320	.065
70	.306	.070
140	.344	.065
$x_{sm} = 0.294\bar{c}$ at M = 1.6		
30	0.755	0.015
50	.960	.030
70	.990	.040
140	.982	.045
$x_{sm} = 0.564\bar{c}$ at M = 1.6		
30	1.50	0.004
50	1.74	.015
70	1.96	.025
140	1.99	.030

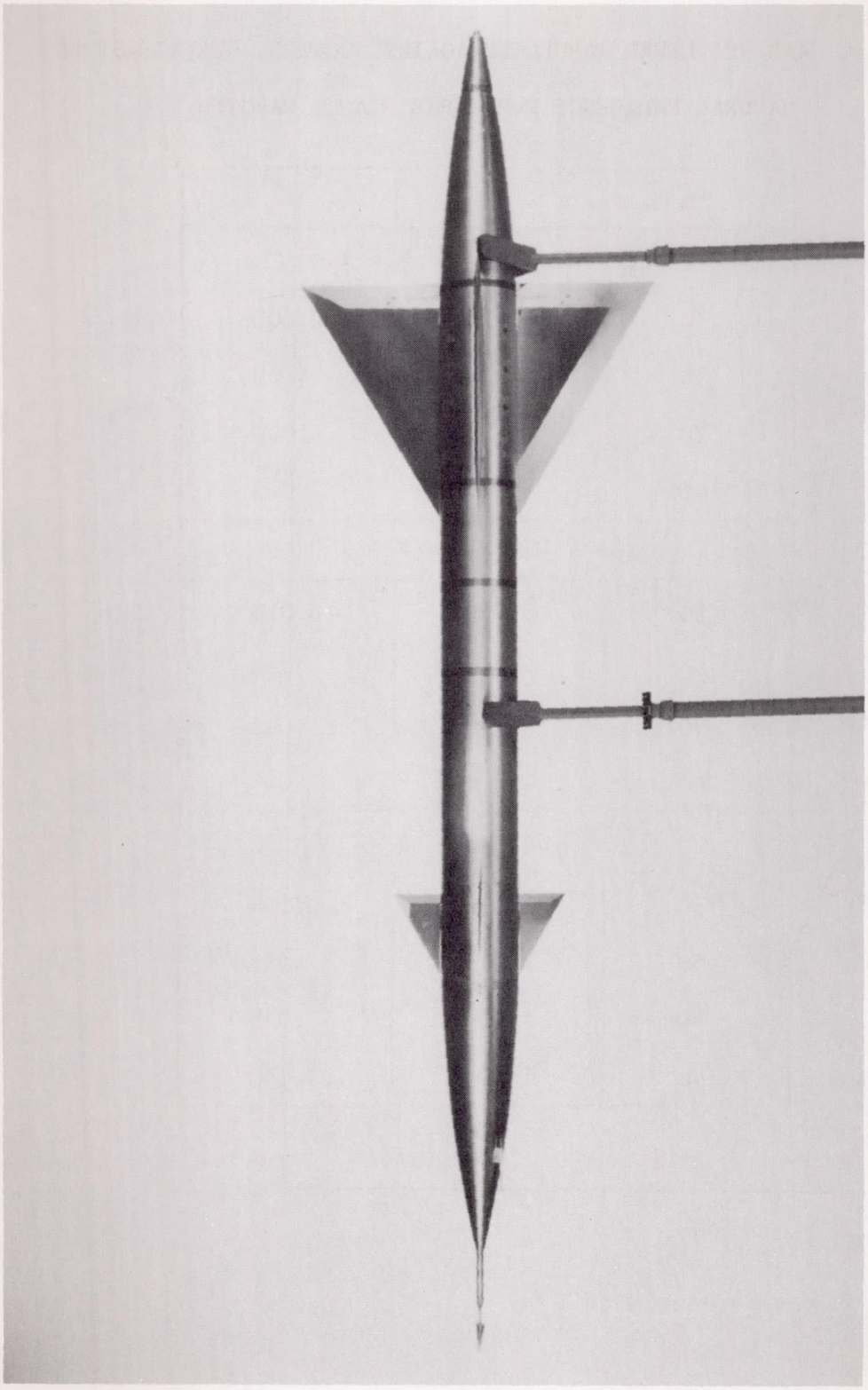

L-67712.1

Figure 1.- Photograph of missile configuration.

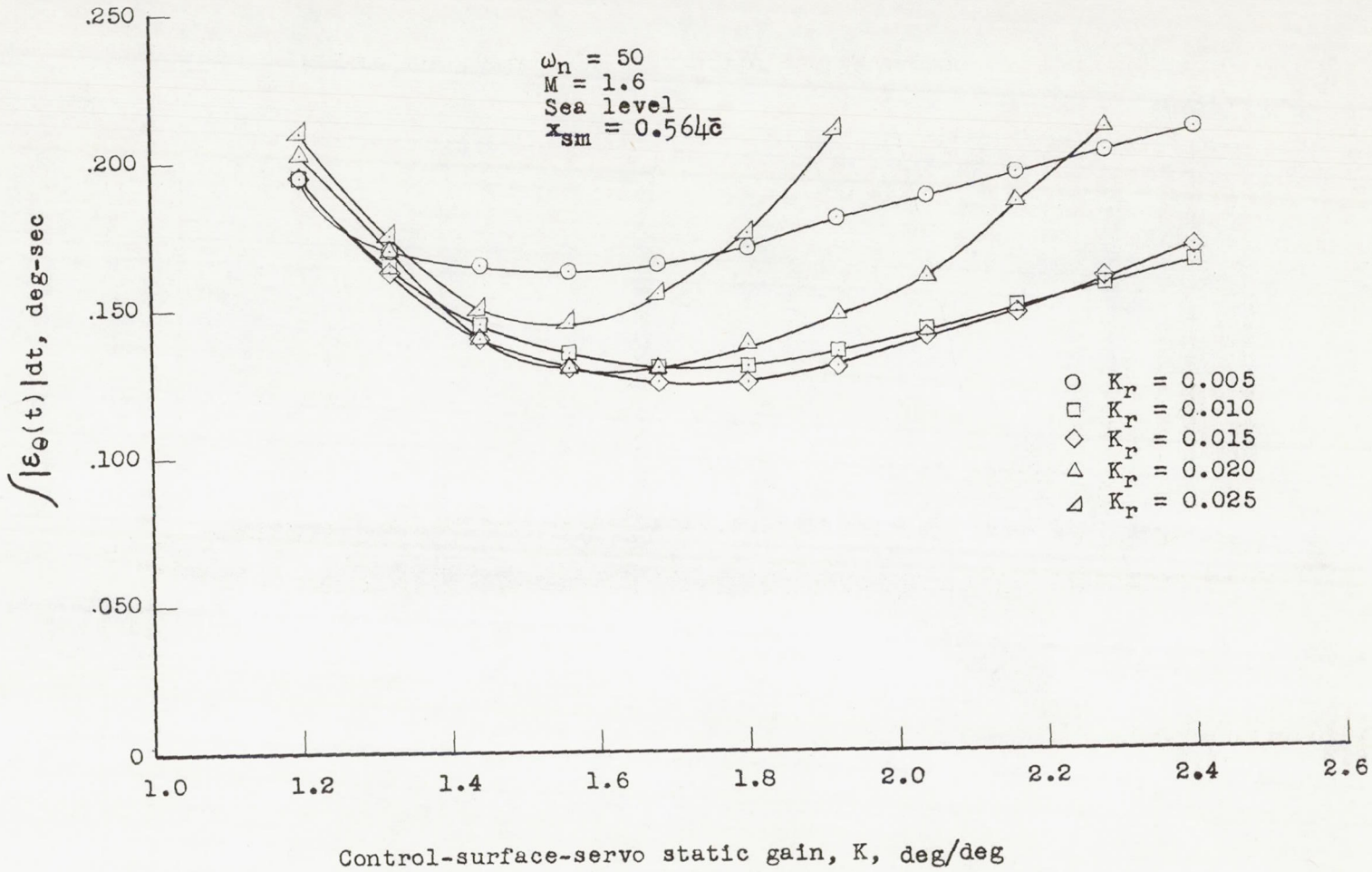

Figure 2.- Parametric contour representation of the surface $\int|\epsilon_\theta(t)|\,dt = F(K, K_r)$ where $\epsilon_\theta(t)$ is obtained from the response to a unit step input $\gamma_i(t)$. x_{sm} is given for $M = 1.6$ at sea level.

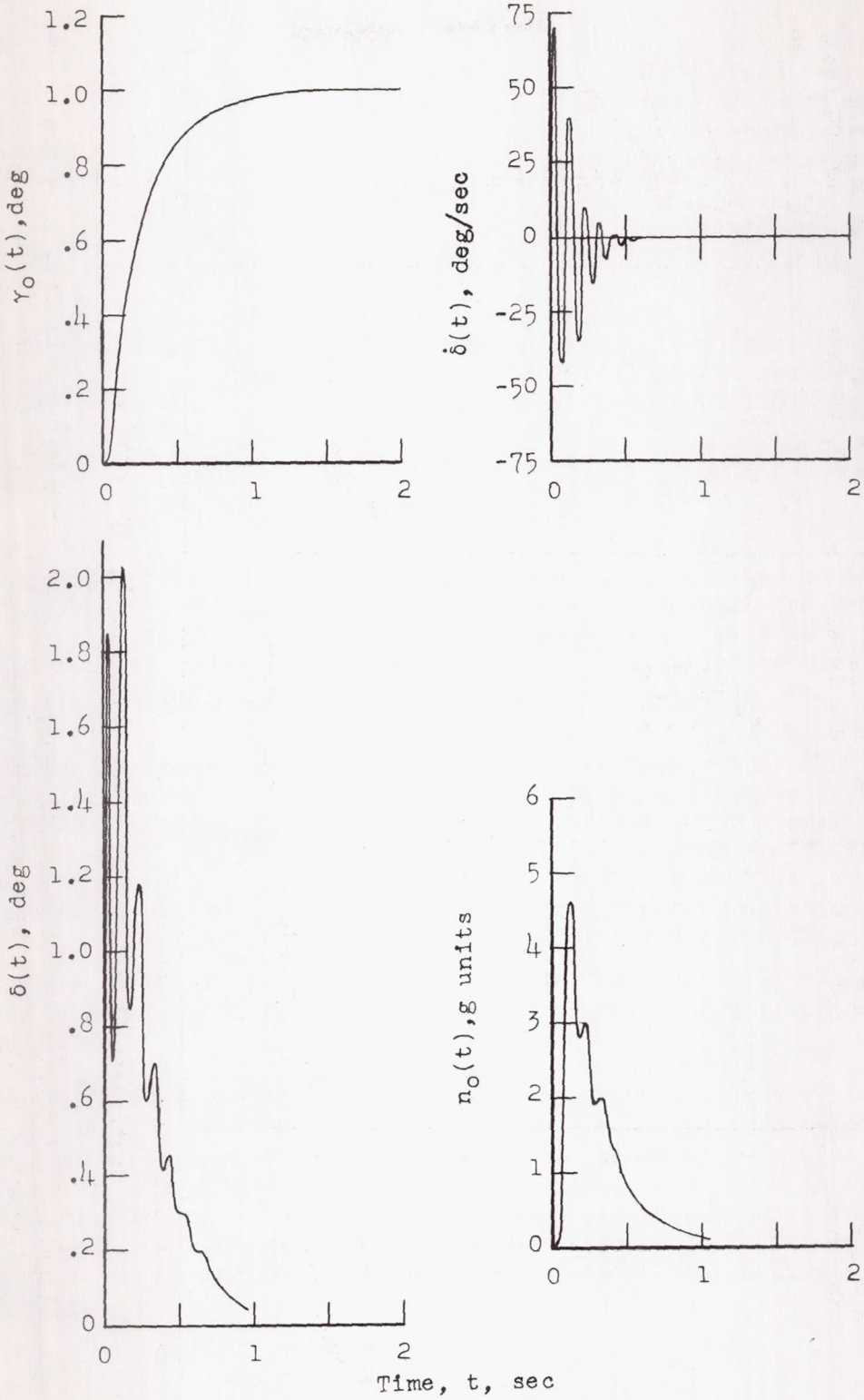

Figure 3.- Sample transient responses to a unit step input for $M = 1.6$ at sea level. $\omega_n = 70$; static margin, $0.564\bar{c}$.

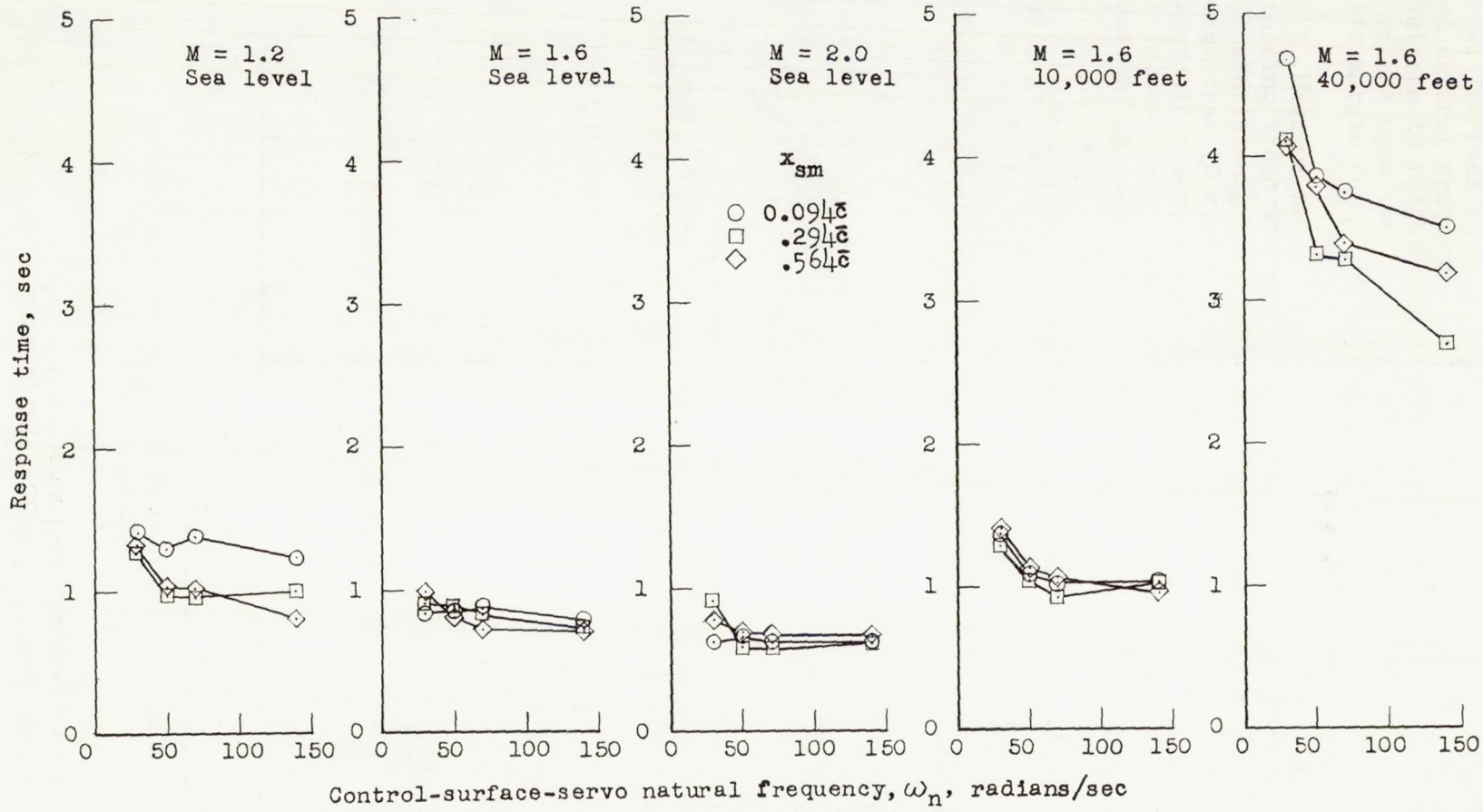

Figure 4.- Response time is plotted against control-surface-servo natural frequency in response to a unit step input $\gamma_i(t)$. x_{sm} is given for M = 1.6 at sea level.

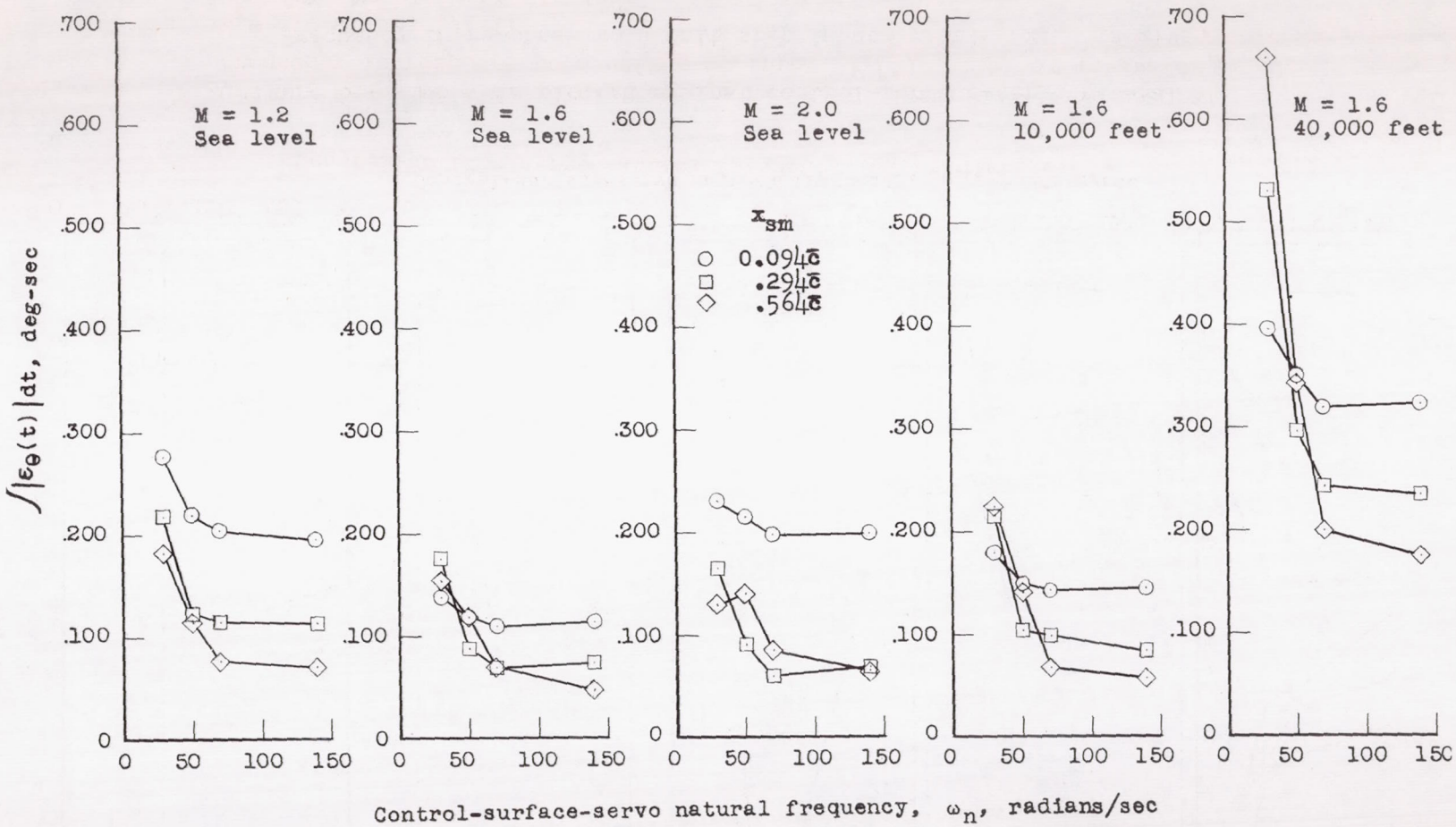

Figure 5.- $\int|\epsilon_\theta(t)|\,dt$ is plotted against control-surface-servo natural frequency in response to a unit step input $\gamma_i(t)$. x_{sm} is given for $M = 1.6$ at sea level.

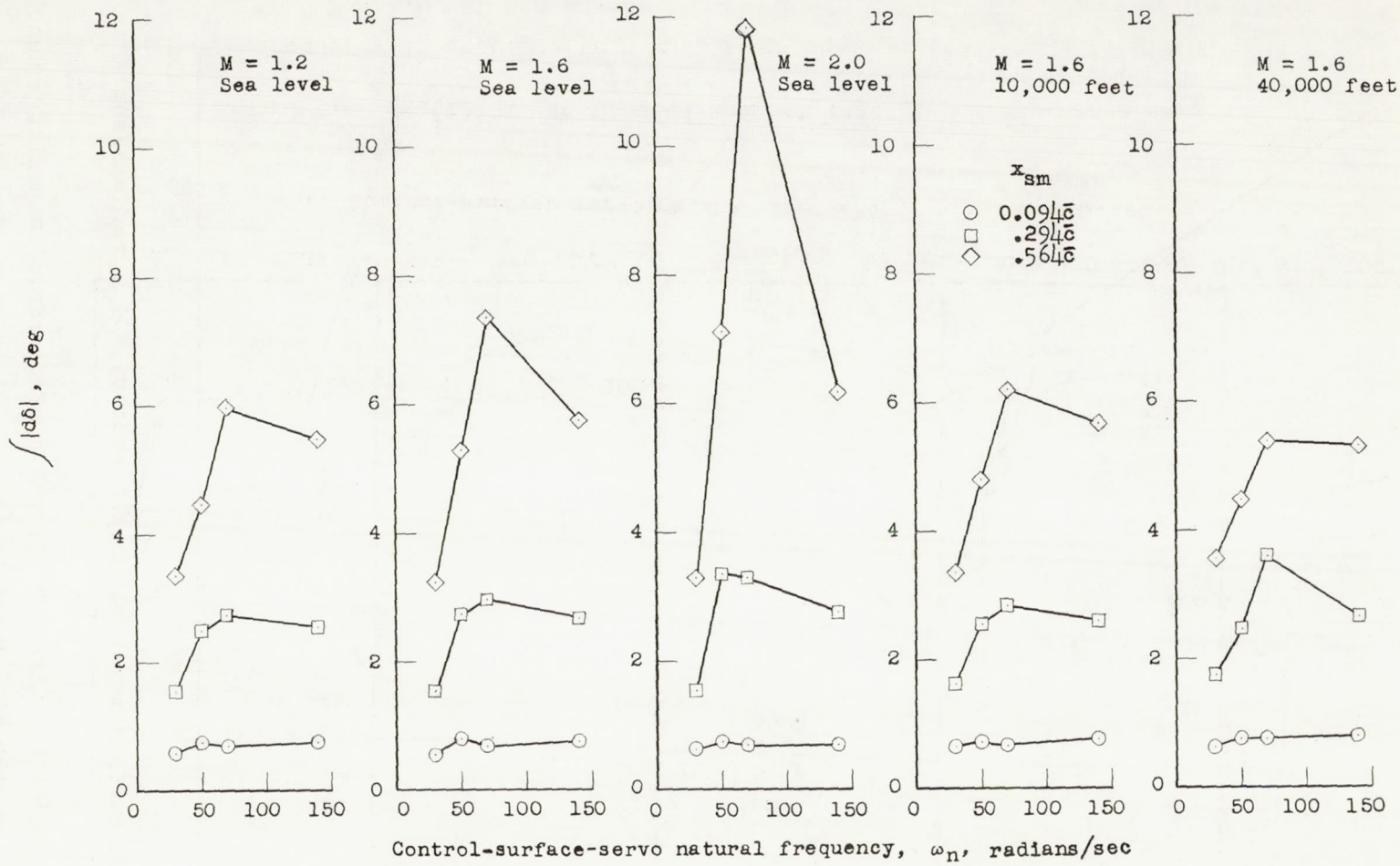

Figure 6.- $\int |d\delta|$ is plotted against control-surface-servo natural frequency in response to a unit step input $\gamma_i(t)$. x_{sm} is given for $M = 1.6$ at sea level.

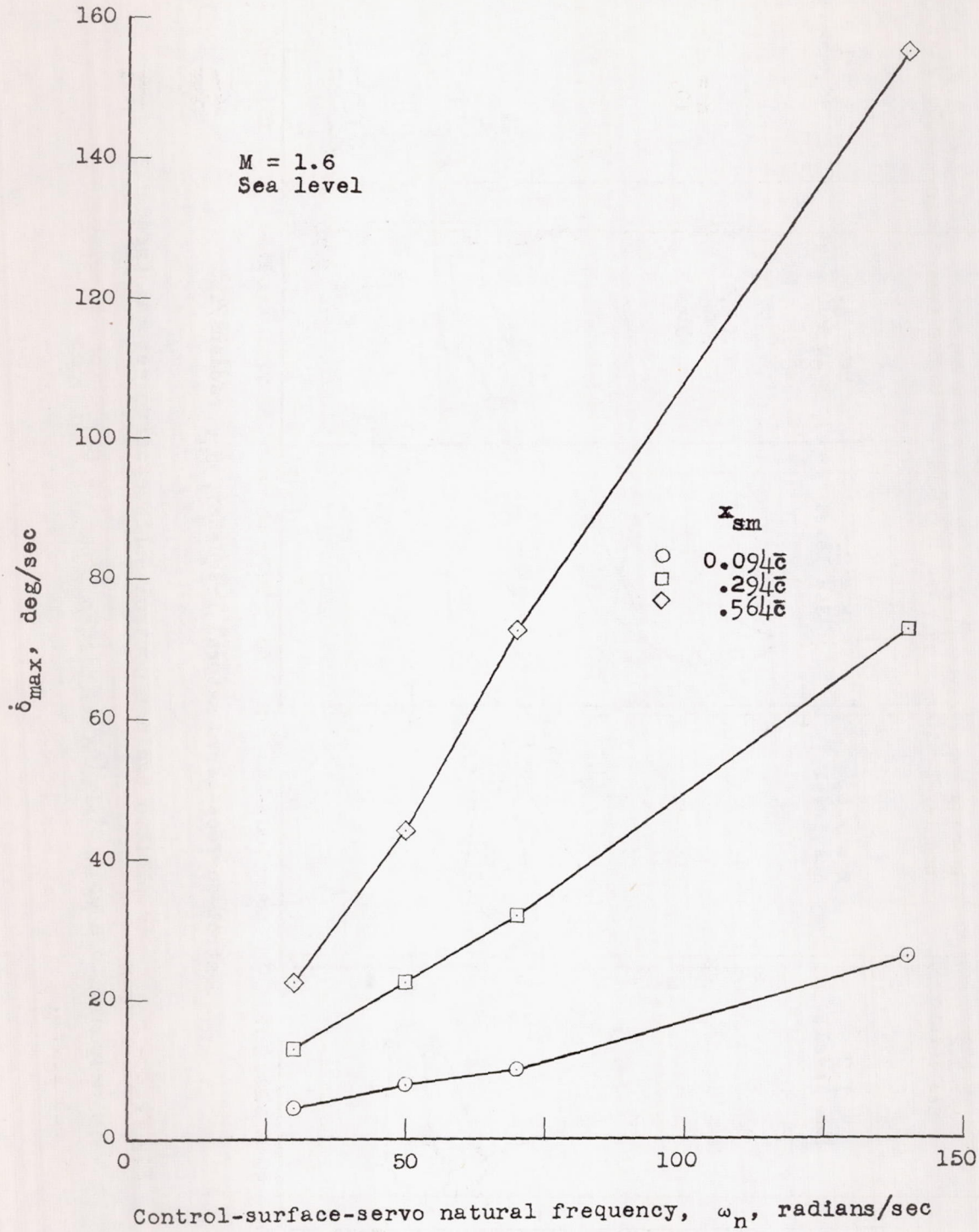

Figure 7.- $\dot{\delta}_{max}$ is plotted against control-surface-servo natural frequency in response to a unit step input $\gamma_i(t)$. x_{sm} is given for $M = 1.6$ at sea level.

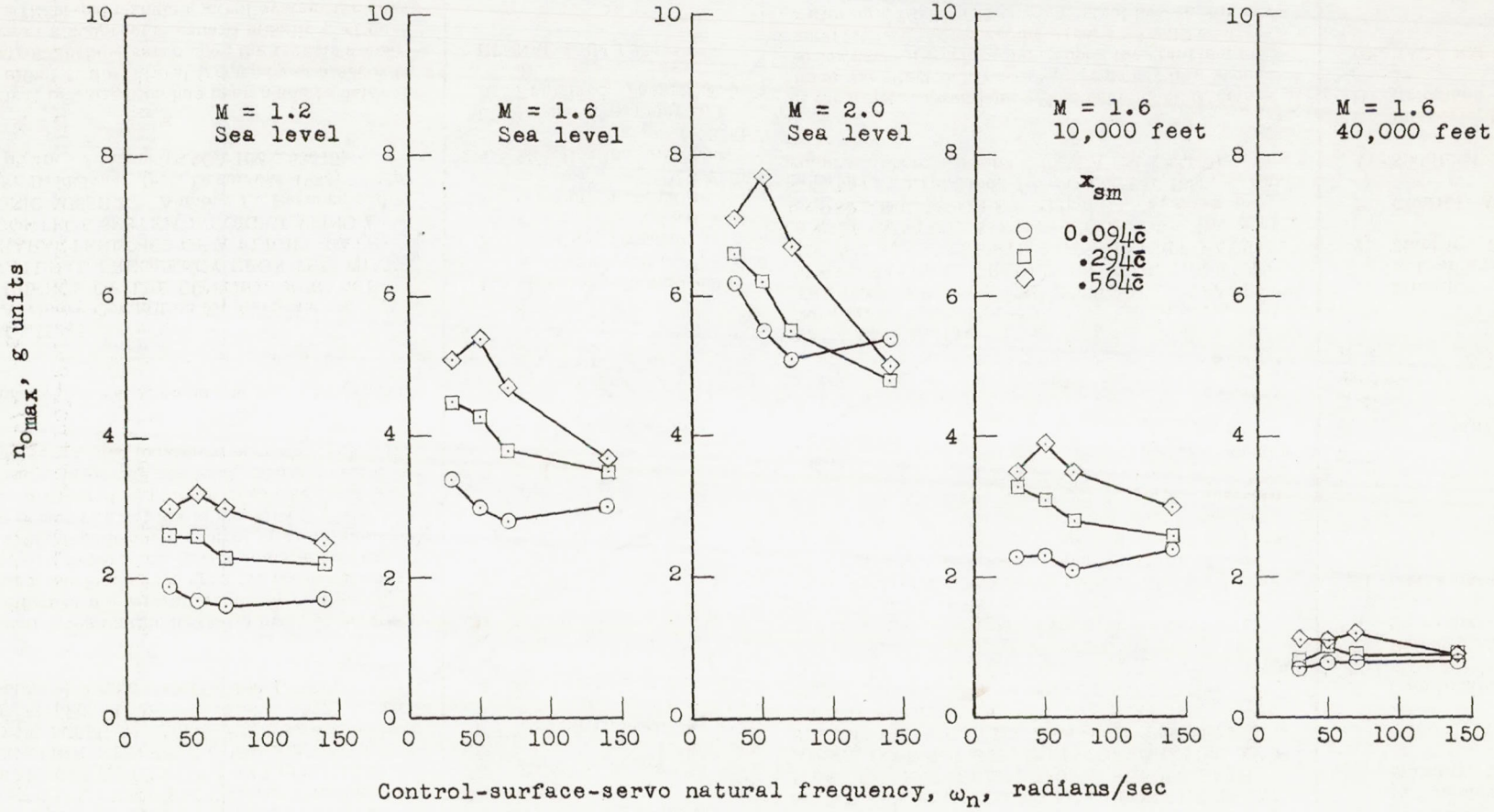

Figure 8.- $n_{o_{max}}$ is plotted against control-surface-servo natural frequency in response to a unit step input $\gamma_i(t)$. x_{sm} is given for $M = 1.6$ at sea level.

NACA-Langley